Theory of laser-amplifier injection locking

J. Jahanpanah and R. Loudon
Physics Department, Essex University, Colchester CO4 3SQ, England
(Received 10 April 1996)

The theory of the laser amplifier is developed for conditions in which the strength of the input signal is increased from small values, where the amplification is linear, to larger values, where the amplification becomes nonlinear. The below-threshold laser amplifier oscillates at a single frequency equal to that of the input signal, and its properties are found by solution of the nonlinear equation of motion for the single excitation amplitude. For the above-threshold laser amplifier, the effects of the nonlinear behavior are to shift the laser frequency from its free-running value and to transfer intensity from the laser line to the signal frequency and to a range of satellite lines, whose frequency detunings are integer multiples of the signal detuning. The intensities of the various emission lines of the laser are calculated by power-series expansions of the field amplitudes up to terms of fourth order in the input signal strength. The onset of injection locking is determined by the conditions for which the intensity at the shifted free-running laser frequency falls to zero. The injection-locked state is characterized by a single excitation frequency equal to that of the input signal, and its properties are found by solution of the same nonlinear equation of motion as for the below-threshold amplifier. The ranges of input signal strength and detuning are determined for which the injection-locked state is stable. The energy conservation properties of the laser amplifier are considered for each of its operating states. [S1050-2947(96)01211-5]

PACS number(s): 42.60.Lh

I. INTRODUCTION

The properties of the single-mode laser amplifier in its regime of linear operation have been studied recently both experimentally and theoretically [1]. The amplification characteristics of an above-threshold argon-ion laser were measured as functions of the laser pumping rate and the detuning ω of the input signal frequency ω_S from the frequency ω_{L0} of the free-running laser emission

$$\omega = \omega_S - \omega_{L0}. \tag{1.1}$$

The results are well accounted for by a theory correct to first order in the amplitude of the weak input signal, consistent with the linear regime of operation of the amplifier. The principal finding of the work is the importance of the excitation of the field in the laser cavity at the image frequency ω_I, detuned from the free-running laser frequency by $-\omega$,

$$\omega_I = \omega_{L0} - \omega. \tag{1.2}$$

The image excitation is produced by a four-wave-mixing process driven by the strongly excited laser mode via pulsations in the population inversion of the laser. It is found that the image field has a magnitude comparable to the signal field but with opposite sign, so that the linear amplification measured by self-heterodyne detection of the laser output suffers from significant cancellation between the beats of the strong laser line with the much weaker image and signal output fields. Thus it is necessary to include the signal and image satellites of the laser line in the theoretical model even for treatments of linear amplification. Substantial image components are also observed in the direct detection of the emission from semiconductor laser amplifiers [2].

If the amplitude of the input signal is now steadily increased, several effects appear. Thus the laser frequency ω_L itself shifts from its free-running value ω_{L0} towards the input signal frequency ω_S, by an amount proportional to the second and higher even powers of the signal amplitude. The amplification of the signal field by the laser begins to depart from linear behavior as the signal and image output amplitudes acquire significant terms in the third and higher odd powers of the input signal amplitude. Furthermore, the excitation spectrum of the cavity acquires additional satellites at frequencies separated from the laser line by higher integer multiples of the signal detuning $\overline{\omega}$ from the shifted laser frequency. These nonlinear contributions and additional satellite lines progressively remove intensity from the laser line as the input signal amplitude increases. The laser intensity is eventually all transferred to the signal, image, and higher-order satellites, the emission at frequency ω_L is extinguished, and the phenomenon of injection locking occurs. With the collapse of the laser excitation, only the signal excitation at frequency ω_S remains and the multiple satellite spectrum disappears. The sequence of spectra, beginning with the image-laser-signal triplet, continuing to larger numbers of satellite lines, and ending with the single spectral component of the injection-locked state, has been clearly observed for the CO_2 laser [3]. The multiple-satellite spectra that occur on the approach to injection locking are discussed and illustrated by Siegman [4].

The theory of injection locking can be approached in two distinct ways, and the main purpose of the present paper is to develop and compare the two approaches. The first approach is to extend our previous calculations [1] by including terms of higher order than the first in the input signal amplitude, so that the nonlinear behavior of the laser amplifier can be described. The aim is to understand the phenomena that occur above threshold as the amplitude of the input is increased from very small values up to the value for which injection locking occurs, and we refer to this regime as the *normal*

state of the amplifier. The simplest extension of our previous work is the inclusion of second-order terms, and these already provide a model of the injection-locking phenomenon, in which a steady increase in the amplitude of the input signal, or a decrease in its detuning, produces a quenching of emission at the laser frequency. A theory of this kind was used by Pantell [5] in his pioneering treatment of injection locking, and some of our results are in qualitative agreement with his. However, the proper inclusion of the image excitation produces quantitative differences even for weak input signals. More complete results are obtained by inclusion of third- and fourth-order terms, and the higher-order theory of the normal state of the laser amplifier provides a more accurate description of the satellites, which remains valid closer to the injection-locking point. This theory must be approximate as it is not practicable to take full account of the increasingly nonlinear behavior in the vicinity of the injection-locking point, manifested by the growing number of different frequencies at which satellites are excited.

The second approach begins with a description of the injection-locked state, which is basically simpler, as the field excitation in the laser cavity has only a single-frequency component determined by the input signal. The theory can be carried through exactly in this case and the laser equations of motion reduce to a cubic equation for the field amplitude [4], which can be solved either approximately or numerically. The theory of the injection-locked state was initially considered by Spencer and Lamb [6], and subsequently there have been many calculations of the properties of the laser with an injected signal [7–10]. Much of this work has been concerned with ranges of the laser parameters for which the output displays varieties of dynamic behavior such as self-pulsing and chaos [11,12]. By contrast, our interest here is in modestly pumped lasers belonging to classes *A* or *B* [13], whose dipole-moment decay rates greatly exceed those of both the cavity field and the atomic population inversion, where these more exotic effects do not occur. This regime of operation has previously been discussed by Arecchi and coworkers [13,14], and our results are extensions of theirs. We obtain the variations in the laser field and atomic inversion with the strength and frequency of the input signal, and we determine the ranges of signal parameters for which the injection-locked state is stable.

Section II summarizes the laser model, with details of the equations of motion and their solutions for the free-running laser, the single-frequency solutions that occur below threshold and in the injection-locked state, and the multiple-frequency solutions that occur in the normal state of the above-threshold laser amplifier. Section III deals with the nonlinear behavior of the below-threshold amplifier when intense signals are incident, by appropriate solution of the same cubic equation as occurs for the injection-locked laser amplifier. Sections IV and V present the theory of the normal state of the amplifier correct to the second, third, and fourth orders in the input signal amplitude respectively. The injection-locked state of the above-threshold laser amplifier is treated in Sec. VI, and the conditions for its stability are determined. The predictions from the two forms of injection-locking theory for the transition between normal and locked states are evaluated in Secs. IV–VI. The calculations cover the properties of the laser with an injected signal in its three distinct states, namely, below threshold, the normal state above threshold, and the injection-locked state above threshold. Particular attention is paid to the conditions of energy balance in these three states, and we identify the ways in which the energy consumed by the amplification process is sourced by reductions in the other forms of output from the laser cavity. The results are discussed in Sec. VII, where the two approaches to the theory of injection locking are compared and experimental tests of the theory are proposed.

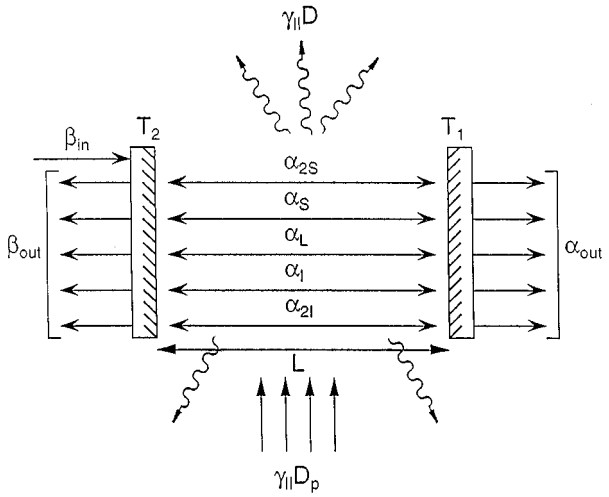

FIG. 1. Representation of the laser cavity showing the notations for mirror transmission coefficients, the input and output photon-flux amplitudes, and the photon-number amplitudes of the various internal frequency components. The laser pump rate $\gamma_{\|}D_p$ and the rate of loss of energy by spontaneous emission in all spatial directions $\gamma_{\|}D$ are also indicated.

II. EQUATIONS OF MOTION

A. Laser model

The basic model is essentially the same as that used in the previous treatment of the regime of linear amplification [1], and only its main features are summarized here. The structure of the laser amplifier cavity is shown in Fig. 1, together with the notation for the laser field α_L, the input signal amplitude $\beta_{\rm in}$, and the amplitudes of the other frequency components of the fields that are generated by the interactions in the cavity. The dimensions of these amplitudes are chosen so that *inside* the cavity quantities such as $|\alpha_L|^2$ give the mean number of photons excited at the relevant frequency, while *outside* the cavity quantities such as $|\beta_{\rm in}|^2$ give the mean photon-number flux, with dimensions of inverse time.

The intensity damping rates from each end of the cavity are related to the intensity transmission coefficients T_1 and T_2 of the mirrors by

$$\gamma_1 = cT_1/2L, \quad \gamma_2 = cT_2/2L, \tag{2.1}$$

so that the total damping rate of the internal *field* in the cavity is given by

$$\gamma_c = (\gamma_1 + \gamma_2)/2. \tag{2.2}$$

The relations between the internal electric field of the cavity α, the input signal β_{in}, and the output fields from each end of the cavity, which is assumed to have a high Q, have the usual forms [15]

$$\alpha_{\text{out}} = \gamma_1^{1/2}\alpha \tag{2.3}$$

on the right and

$$\beta_{\text{out}} = \gamma_2^{1/2}\alpha - \beta_{\text{in}} \tag{2.4}$$

on the left, where the field emitted from the cavity is superposed on the reflected input field. These relations are important for demonstrations of the energy conservation law of the laser amplifier.

The interactions between the optical and atomic components of the laser in the presence of an input signal determine the forms of the three important laser parameters: the cavity field α, the atomic population inversion D, and the atomic dipole moment d. The behaviors of these parameters are obtained by solution of the Maxwell-Bloch equations in the forms [4,16,17]

$$\dot{\alpha} + (\gamma_c + i\omega_{L0})\alpha = gd + \gamma_2^{1/2}\beta_{\text{in}}, \tag{2.5}$$

$$\dot{D} + \gamma_{\parallel} D = \gamma_{\parallel} D_p - g(\alpha^* d + \alpha d^*), \tag{2.6}$$

and

$$\dot{d} + (\gamma_{\perp} + i\omega_{L0})d = g\alpha D, \tag{2.7}$$

where g is the coupling constant between the dipole moment of the atoms and the cavity electric field; $\gamma_{\parallel}$, $\gamma_{\perp}$, and γ_c are, respectively, the population-inversion decay rate, the dipole-moment decay rate, and the total damping rate of the internal field in the cavity defined in (2.2); ω_{L0} is the frequency of the free-running laser; D_p measures the laser pumping rate in terms of the mean population inversion that would be achieved in the absence of any optical field in the cavity; and β_{in} is the input signal amplitude coupled into the laser cavity as shown schematically in Fig. 1. The equation of motion for the population inversion takes the simple form (2.6) only for laser transitions in which the lower-level population is negligible. Figure 1 also includes representations of the rate $\gamma_{\parallel} D_p$ at which the pump supplies energy to the inverted population and the rate $\gamma_{\parallel} D$ at which energy radiates out of the cavity in all directions by the process of spontaneous emission.

For class-A and class-B lasers, the dipole moment decay rate is very much larger than the population inversion and cavity decay rates ($\gamma_{\perp} \gg \gamma_{\parallel}, \gamma_c$) and the effects of homogeneous collision broadening overcome those of the inhomogeneous Doppler broadening. Thus spectral hole-burning effects are negligible and Eq. (2.7) can be approximated by

$$\gamma_{\perp} d = g\alpha D. \tag{2.8}$$

This expression can be substituted for d in (2.5) and (2.6), which then provide the pair of equations

$$\dot{\alpha} + (\gamma_c + i\omega_{L0})\alpha = (g^2/\gamma_{\perp})\alpha D + \gamma_2^{1/2}\beta_{\text{in}} \tag{2.9}$$

and

$$\dot{D} + \gamma_{\parallel} D = \gamma_{\parallel} D_p - (2g^2/\gamma_{\perp})|\alpha|^2 D \tag{2.10}$$

to be solved for the motion of the laser system. The lasing atoms are assumed to be sufficiently mobile that spatial hole-burning effects are also negligible.

B. Energy conservation

It is simply shown from (2.9) and its complex conjugate that

$$d|\alpha|^2/dt = -2\gamma_c|\alpha|^2 + (2g^2/\gamma_{\perp})|\alpha|^2 D + \gamma_2^{1/2}(\alpha\beta_{\text{in}}^* + \alpha^*\beta_{\text{in}}), \tag{2.11}$$

and addition of this equation to (2.10) gives

$$d(|\alpha|^2 + D)/dt = -2\gamma_c|\alpha|^2 + \gamma_{\parallel}(D_p - D) + \gamma_2^{1/2}(\alpha\beta_{\text{in}}^* + \alpha^*\beta_{\text{in}}). \tag{2.12}$$

The quantity differentiated on the left is proportional to the total excitation energy in the laser cavity, including the contributions from the electromagnetic field and the inverted atoms. The laser steady-state condition can therefore be written

$$2\gamma_c|\alpha|^2 - \gamma_2^{1/2}(\alpha\beta_{\text{in}}^* + \alpha^*\beta_{\text{in}}) + \gamma_{\parallel} D = \gamma_{\parallel} D_p, \tag{2.13}$$

and this is transformed with the use of (2.2)–(2.4) into

$$\overline{|\alpha_{\text{out}}|^2} + \overline{|\beta_{\text{out}}|^2} + \gamma_{\parallel}\overline{D} = \gamma_{\parallel} D_p + |\beta_{\text{in}}|^2, \tag{2.14}$$

where the overbars denote cycle-averaged mean values that are appropriate when the fields and population inversion contain several frequency components.

These equations express energy conservation in the laser system. Thus upon multiplication of (2.14) by $\hbar\omega_L$ and with neglect of the small frequency differences between the various field components, the terms on the left are, respectively, the mean energy fluxes leaving the cavity through its two mirrors and the rate of spontaneous emission of radiative energy in all directions by the inverted atoms, while the terms on the right are the rates at which the pump and the input signal supply energy to the system. It is shown in subsequent sections that the energy conservation condition is indeed satisfied for the various states of the laser.

C. Free-running laser

In the absence of any input signal, the cavity field has the single-frequency form

$$\alpha = \alpha_L \exp(-i\omega_{L0}t) \tag{2.15}$$

and the population inversion D is independent of the time. The solutions of (2.9) and (2.10) for these quantities are either

$$\alpha = \alpha_L = 0, \quad D = D_p, \tag{2.16}$$

corresponding to the laser below threshold, or

$$|\alpha|^2 = |\alpha_L|^2 = \left(\frac{D_p}{D_0} - 1\right)\frac{\gamma_{\perp}\gamma_{\parallel}}{2g^2} = (C-1)n_s \tag{2.17}$$

and

$$D=\gamma_c\gamma_\perp/g^2\equiv D_0, \tag{2.18}$$

corresponding to the laser above threshold. Here

$$C=D_p/D_0=g^2D_p/\gamma_c\gamma_\perp \tag{2.19}$$

is the cooperation parameter, or normalized pumping rate, equal to unity at threshold, and

$$n_s=\gamma_\perp\gamma_\parallel/2g^2 \tag{2.20}$$

is the saturation photon number, equal to the mean number of photons in the laser cavity at twice the threshold pumping rate $C=2$. It is seen from (2.19) that for this degree of laser excitation, the constant above-threshold population inversion D_0 has one-half of its value D_p in the absence of any optical field and n_s thus characterizes the cavity photon number for which significant saturation of the active atomic excited states begins to occur. The phase of the cavity field α_L is not determined by the equations of motion.

The stability of the solutions of the laser equations of motion is determined in the usual way [11], by assuming that small displacements $\delta\alpha$ and δD of the cavity field and population inversion from their equilibrium values evolve with a time dependence $\exp(\lambda t)$. The equilibrium values are then stable if the damping constants λ obtained from the equations of motion are all negative. With two dynamical variables, there are two values of λ determined by a quadratic equation. It is found in this way that the solution (2.16) has damping constants

$$\lambda=-\gamma_\parallel,-\gamma_c(1-C), \tag{2.21}$$

and it is therefore stable below threshold $C<1$. The solution (2.17) has damping constants [13,14]

$$\lambda=-\frac{\gamma_\parallel C}{2}\pm\left\{\frac{\gamma_\parallel^2C^2}{4}-2\gamma_\parallel\gamma_c(C-1)\right\}^{1/2}, \tag{2.22}$$

and it is therefore stable above threshold $C>1$.

With no input signal, the energy conservation condition (2.13) reduces to

$$2\gamma_c|\alpha_L|^2=\gamma_\parallel(D_p-D), \tag{2.23}$$

and it is seen that this is satisfied both by the solution (2.16) below threshold and the solutions (2.17) and (2.18) above threshold. The energy balance between the laser input and output is illustrated as a function of cooperation parameter in Fig. 2. Thus the rate at which the pump supplies energy to the inverted population is equal to $\gamma_\parallel D_p$ at all values of C. Above threshold $C>1$, the inverted atoms emit light into the laser mode at a rate given by (2.23). This total rate can be divided into contributions from stimulated and spontaneous emission, whose ratio is given as usual by the mean number of photons $|\alpha_L|^2$ in the mode [18], so that

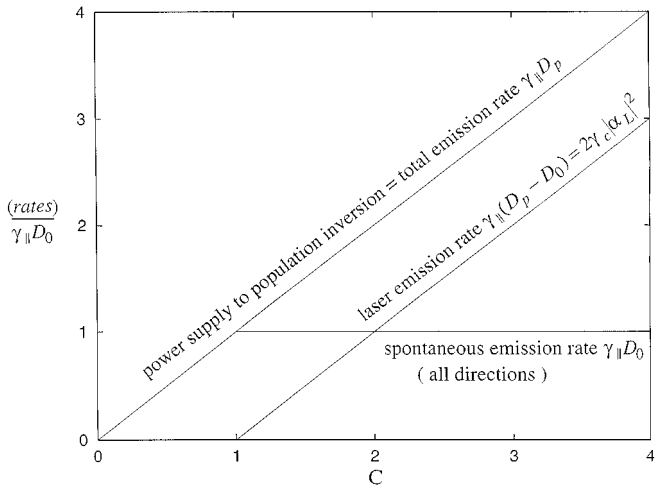

FIG. 2. Energy balance in the free-running laser showing the rates of energy input from the pump, spontaneous emission in all directions, and emission into the laser mode as functions of the cooperation parameter C.

$$\gamma_\parallel(D_p-D_0)=2\gamma_c|\alpha_L|^2=\frac{2\gamma_c|\alpha_L|^2}{|\alpha_L|^2+1}+\frac{2\gamma_c|\alpha_L|^4}{|\alpha_L|^2+1}$$
$$\approx 2\gamma_c(\text{spontaneous})+2\gamma_c|\alpha_L|^2(\text{stimulated}), \tag{2.24}$$

since normally $|\alpha_L|^2\gg 1$. The spontaneous component of the emission into the lasing mode is therefore negligible. The remaining emission by the inverted atoms, at a rate $\gamma_\parallel D$, occurs spontaneously into all other spatial modes; this accounts for all of the emission from the cavity below threshold, while above threshold the spontaneous component remains fixed at its threshold value and the balance of the energy supplied by the pump appears in the lasing mode.

D. Single-frequency solutions

The presence of a nonzero input signal normally excites a multiple-frequency field in the laser cavity and the population inversion generally contains components that oscillate at the differences of these field frequencies. However, the amplifier dynamics retain simple forms for the two cases of the laser amplifier below threshold and the injection-locked laser amplifier above threshold. These states share the feature that the field inside the laser cavity has a single-frequency component determined by the frequency of the input signal. Thus with the input signal field taken in the form

$$\beta_{\text{in}}=\beta_S\exp(-i\omega_St)=\beta_S\exp[-i(\omega_{L0}+\omega)t], \tag{2.25}$$

the mean internal field in the laser cavity can be written

$$\alpha=\alpha_S\exp[-i(\omega_{L0}+\omega)t] \tag{2.26}$$

and the population inversion D is again a static quantity. The equations of motion (2.9) and (2.10) thus provide a pair of simultaneous equations that can be solved for the two unknowns α_S and D.

Consider first the field equation (2.9), which gives

$$[\gamma_c-(g^2/\gamma_\perp)D-i\omega]\alpha_S=\gamma_2^{1/2}\beta_S. \tag{2.27}$$

The complex fields are conveniently expressed in terms of amplitudes and phase angles according to

$$\alpha_S=|\alpha_S|e^{i\phi_S},\quad \beta_S=|\beta_S|e^{i\phi_{\rm in}}. \tag{2.28}$$

The imaginary part of (2.27) then gives

$$\omega|\alpha_S|=\gamma_2^{1/2}|\beta_S|\sin(\phi_S-\phi_{\rm in}), \tag{2.29}$$

while its square modulus is

$$\{[\gamma_c-(g^2/\gamma_\perp)D]^2+\omega^2\}|\alpha_S|^2=\gamma_2|\beta_S|^2. \tag{2.30}$$

The two terms in the curly brackets on the left-hand side of this equation are both positive, and it follows that the magnitude of the cavity field produced by an input signal of given amplitude and detuning satisfies the inequality

$$|\alpha_S|\leqslant\gamma_2^{1/2}|\beta_S|/|\omega|. \tag{2.31}$$

The value of $|\alpha_S|$ thus reduces with increase in the detuning $|\omega|$ so that the magnitude of the sine in (2.29) is properly less than or equal to unity for all input signal parameters.

The corresponding solution of the population inversion equation of motion (2.10) is

$$D=\frac{CD_0}{1+(|\alpha_S|^2/n_s)}, \tag{2.32}$$

where D_0, C, and n_s are defined in (2.18), (2.19), and (2.20) respectively. Insertion of this solution into (2.30) gives

$$\left\{\gamma_c^2\left(\frac{|\alpha_S|^2+(1-C)n_s}{|\alpha_S|^2+n_s}\right)^2+\omega^2\right\}|\alpha_S|^2=\gamma_2|\beta_S|^2. \tag{2.33}$$

This cubic equation determines the cavity field strengths $|\alpha_S|$ for the below-threshold ($C<1$) and injection-locked ($C>1$) laser amplifiers as functions of the input signal parameters [4]. Note that the population inversion decay rate $\gamma_\parallel$ appears only implicitly in the saturation photon number in (2.32) and (2.33) so that, for a given value of n_s, the same forms of variation of $|\alpha_S|$ and D with the input signal amplitude $|\beta_S|$ occur for class-A and class-B lasers.

The system mimics a free-running laser when (2.31) is satisfied as an equality, and the values of the amplifier variables obtained from (2.29), (2.30), and (2.33) are then

$$\phi_S-\phi_{\rm in}=\pm\pi/2,\quad D=D_0,\quad |\alpha_S|^2=(C-1)n_s, \tag{2.34}$$

for $|\alpha_S|=\gamma_2^{1/2}|\beta_S|/|\omega|$, where these solutions are valid only above threshold ($C>1$). The 90° phase difference between the input and cavity fields ensures that there is no interference between the two contributions in the output field given by (2.4). The output fluxes are thus the same as those for the free-running laser, ignoring the small difference between the frequencies ω_S and ω_L, plus an additional output equal to the input signal flux on the left of the cavity shown in Fig. 1.

The stability of the single-frequency solutions is determined by the method outlined in Sec. II C. However, both the phase and the amplitude of the cavity field need to be evaluated in the presence of an input signal and, together with the population inversion, there is now a total of three dynamical variables. The damping constants λ are thus determined by solution of a cubic equation

$$a_0+a_1\lambda+a_2\lambda^2+\lambda^3=0, \tag{2.35}$$

where the coefficients are found, consistent with previous work [14], to be

$$a_0=\gamma_\parallel\gamma_c^2\left(1-\frac{D}{D_0}\right)^2\left(1+\frac{|\alpha_S|^2}{n_s}\right)+2\gamma_\parallel\gamma_c^2\times\left(1-\frac{D}{D_0}\right)\frac{D}{D_0}\frac{|\alpha_S|^2}{n_s}+\omega^2\gamma_\parallel\left(1+\frac{|\alpha_S|^2}{n_s}\right), \tag{2.36}$$

$$a_1=2\gamma_\parallel\gamma_c\left(1-\frac{D}{D_0}\right)\left(1+\frac{|\alpha_S|^2}{n_s}\right)+\gamma_c^2\left(1-\frac{D}{D_0}\right)^2+2\gamma_\parallel\gamma_c\frac{D}{D_0}\frac{|\alpha_S|^2}{n_s}+\omega^2, \tag{2.37}$$

and

$$a_2=\gamma_\parallel\left(1+\frac{|\alpha_S|^2}{n_s}\right)+2\gamma_c\left(1-\frac{D}{D_0}\right). \tag{2.38}$$

The mean intracavity photon number $|\alpha_S|^2$ and atomic population inversion D are related by (2.32), and these coefficients can thus be expressed in terms of a single equilibrium variable.

The conditions for stability are now obtained from Hurwitz's theorem [19], which states that the roots of (2.35) all have negative real parts if

$$a_0>0,\quad a_1>0,\quad a_2a_1>a_0. \tag{2.39}$$

The cubic equation (2.35) depends implicitly on the input signal amplitude β_S via $|\alpha_S|^2$ and D. It continues to hold in the absence of any input, and the damping constants for the free-running laser given in (2.21) and (2.22) can be rederived for $\omega=0$ by insertion of the equilibrium values of $\alpha_S=\alpha$ and D, given by (2.16) below threshold and (2.17) and (2.18) above threshold. The solutions of (2.33) and their stability conditions (2.39) for below-threshold and injection-locked laser amplifiers are treated in Secs. III and VI, respectively.

E. Multiple-frequency solutions

The solutions of the equations of motion are much more complicated when laser and input signal oscillations of different frequencies are excited simultaneously in the cavity. One consequence, caused by the synchronism effects of the signal and laser oscillators [4,20], is a frequency shift of the laser emission of magnitude denoted ω_L'', correct to second order in the input signal amplitude, so that the shifted frequency is

$$\omega_L=\omega_{L0}+\omega_L''. \tag{2.40}$$

For a class-A laser, where $\gamma_\parallel\gg\gamma_c$, the frequency is shown in Sec. IV to be always pulled towards the input signal fre-

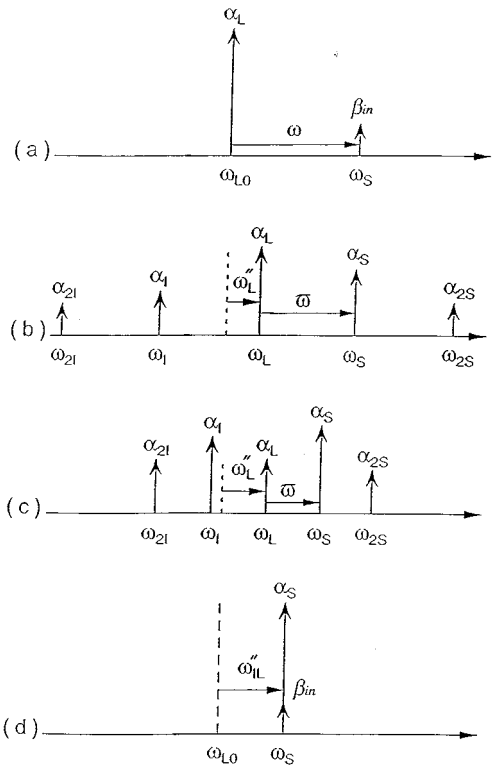

FIG. 3. Schematic representations of the frequency components excited in the laser amplifier: (a) uncoupled free-running laser and input signal; (b) coupled laser and signal showing formation of image and signal satellites; (c) same as (b), but with reduced signal detuning, showing the approach to injection locking; and (d) the injection-locking point.

quency, i.e., the shift is positive when the frequency detuning is positive and negative when the detuning is negative. However, negative frequency shifts, or frequency pushing, can occur for class-*B* lasers at higher positive detunings. Figure 3 schematically shows the laser frequency shift due to synchronization effects, the image and signal satellite lines produced by four-wave-mixing (FWM) processes, and the injection-locking phenomena. Thus, in second order, the frequency relation (1.1) continues to define the signal detuning ω from the *unshifted* emission line of the free-running laser, and this is the primary parameter that characterizes a measurement on the laser amplifier with a fixed signal frequency. However, in identifying the frequency components in the cavity field and the population inversion, it is more convenient to work with the detuning $\overline{\omega}$ from the *shifted* laser line,

$$\overline{\omega}=\omega-\omega_L''=\omega_S-\omega_L=\omega_L-\omega_I, \tag{2.41}$$

where $\overline{\omega}$ varies with the signal strength. The input signal field can be written in the equivalent forms

$$\beta_{\rm in}=\beta_S\exp[-i(\omega_{L0}+\omega)t]=\beta_S\exp[-i(\omega_L+\overline{\omega})t]. \tag{2.42}$$

The expression (1.2) for the image frequency is valid only for weak input signals, where ω_L'' is negligible.

In the first-order approximation, the FWM interaction between the internal strong field of the laser at frequency ω_L and the amplified input signal field (the signal satellite line) at frequency $\omega_L+\overline{\omega}$ always requires the production of a new optical field component (the image satellite line) at frequency $\omega_L-\overline{\omega}$ [1]. The second-order approximation is considered in Sec. IV, where the input signal is assumed sufficiently strong for the first image and signal satellite fields, with modified frequencies given by (2.41), to contribute in other FWM interactions with the strong field of the laser to produce observable signal and image satellite lines at frequencies $\omega_L+2\overline{\omega}$ and $\omega_L-2\overline{\omega}$. Thus, correct to second order in the amplitude of the input signal, the mean internal field of the laser amplifier cavity includes five frequency components to give a total field

$$\begin{aligned}\alpha=&(\alpha_L+\alpha_L'')\exp[-i\omega_L t]+\alpha_S\exp[-i(\omega_L+\overline{\omega})t]\\&+\alpha_I\exp[-i(\omega_L-\overline{\omega})t]+\alpha_{2S}\exp[-i(\omega_L+2\overline{\omega})t]\\&+\alpha_{2I}\exp[-i(\omega_L-2\overline{\omega})t],\end{aligned} \tag{2.43}$$

where α_L'', of the second order in β_S, is the change in the laser field corresponding to energy transferred to the first image and signal ($\alpha_L\alpha_L''^{*}+\alpha_L^{*}\alpha_L''$) and the second image and signal ($|\alpha_L''|^2$) satellite lines. The second and third parts of Fig. 3 show the series of excitation frequencies, with equal separations $\overline{\omega}$, centered on the shifted laser line at ω_L, and a similar spectrum is also illustrated in [4].

The mean population inversion of the atoms also contains five frequency components in the form

$$\begin{aligned}D=&D_0+D_0''+D_1\exp(-i\overline{\omega t})+D_1^{*}\exp(i\overline{\omega t})\\&+D_2\exp(-2i\overline{\omega t})+D_2^{*}\exp(2i\overline{\omega t}),\end{aligned} \tag{2.44}$$

where D_0 is the static population inversion of the laser in the absence of any input signal, D_1 and D_2 describe the population pulsations to first and second orders in the input signal amplitude, and D_0'' is the second-order change in the static population inversion. The expressions (2.43) and (2.44) can be written in various equivalent forms in terms of the unshifted laser frequency ω_{L0}, the frequency shift ω_L'', and the fixed experimental detuning ω, with the use of (2.40) and (2.41).

III. BELOW-THRESHOLD LASER AMPLIFIER

When the laser is operated below threshold, there is no internal strong coherent field α_L at the resonance frequency ω_{L0}. The cavity field therefore oscillates at the single frequency ω_S of the input signal and the population inversion D is independent of the time. The theory outlined in Sec. II D applies, with C taken to be smaller than unity.

Consider first the magnitude of the cavity field, determined by solution of the cubic equation (2.33). Figure 4 shows some numerical solutions for the cavity photon number $|\alpha_S|^2$ as a function of the input flux $|\beta_S|^2$ for various values of the signal detuning, where the optical strengths are normalized by the saturation photon number defined in (2.20). The solution of (2.33) is easily expanded in a power series for small values of $|\beta_S|^2/\gamma_c n_s$ and the first two terms are

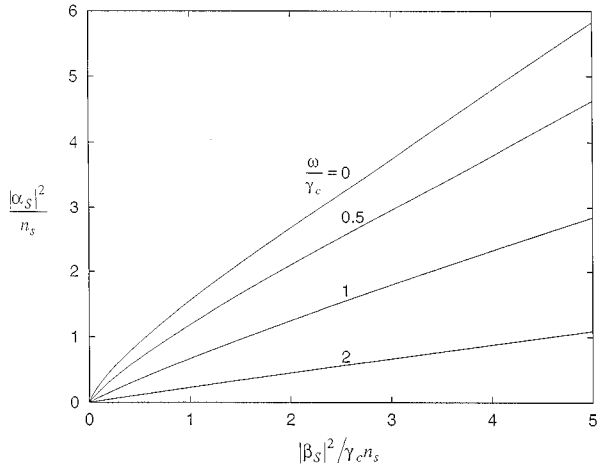

FIG. 4. Normalized cavity mean photon number as a function of the normalized input flux at the signal detunings ω/γ_c indicated, for a below-threshold amplifier ($C=\frac{1}{2}$) and a symmetrical cavity ($\gamma_1=\gamma_2=\gamma_c$).

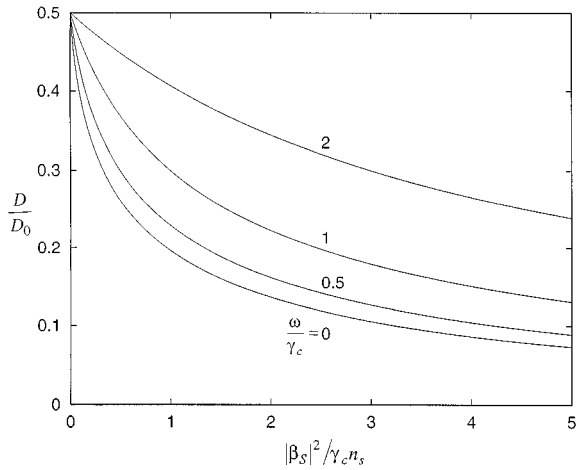

FIG. 5. Normalized population inversion for the same parameters as in Fig. 4.

$$|\alpha_S|^2=\frac{\gamma_2|\beta_S|^2}{\omega^2+\gamma_c^2(1-C)^2}-\frac{2\gamma_2^2\gamma_c^2C(1-C)|\beta_S|^4}{n_s[\omega^2+\gamma_c^2(1-C)^2]^3}$$

$$(|\beta_S|^2\ll\gamma_c n_s), \quad (3.1)$$

where the first term agrees with the result of first-order theory [1] and the second term shows the beginning of nonlinear behavior as the strength of the input signal increases. The cubic equation also has a simple approximate solution in the opposite limit of very high input intensity, where [6]

$$|\alpha_S|^2\approx\frac{\gamma_2|\beta_S|^2}{\omega^2+\gamma_c^2} \quad (|\beta_S|^2\gg\gamma_c n_s), \quad (3.2)$$

and the amplifier again shows linear behavior, as is also evident from Fig. 4.

The corresponding gains in transmission and reflection are defined by

$$G_T(\omega)=\left|\frac{\alpha_{\text{out}}}{\beta_{\text{in}}}\right|^2=\frac{\gamma_1|\alpha_S|^2}{|\beta_S|^2} \quad (3.3)$$

and

$$G_R(\omega)=\left|\frac{\beta_{\text{out}}}{\beta_{\text{in}}}\right|^2=\left|\frac{\gamma_2^{1/2}\alpha_S}{\beta_S}-1\right|^2, \quad (3.4)$$

respectively. The linear transmission gain at low input intensity is obtained from (3.1) as

$$G_T(\omega)=\frac{\gamma_1\gamma_2}{\omega^2+\gamma_c^2(1-C)^2} \quad (|\beta_S|^2\ll\gamma_c n_s), \quad (3.5)$$

in agreement with [1], and the linear gain at high intensity is obtained from (3.2) as

$$G_T(\omega)=\frac{\gamma_1\gamma_2}{\omega^2+\gamma_c^2} \quad (|\beta_S|^2\gg\gamma_c n_s). \quad (3.6)$$

The population inversion is obtained from (2.32), and some numerical results are shown in Fig. 5, where D is normalized by the laser population inversion D_0. The first two terms in the power series expansion of (2.32) for low input intensities give

$$D=CD_0\left\{1-\frac{\gamma_2|\beta_S|^2}{n_s[\omega^2+\gamma_c^2(1-C)^2]}\right\} \quad (|\beta_S|^2\ll\gamma_c n_s), \quad (3.7)$$

while the limit of high input intensities gives a population inversion

$$D\approx CD_0\frac{n_s(\omega^2+\gamma_c^2)}{\gamma_2|\beta_S|^2} \quad (|\beta_S|^2\gg\gamma_c n_s). \quad (3.8)$$

It is evident that the atomic transition is significantly saturated at small detunings and high input signal intensities, and this is the cause of the falloff in transmission gain from the low-intensity form (3.5) to the high-intensity form (3.6). The saturation of the population inversion also causes a reduction in the rate $\gamma_\parallel D$ of spontaneous emission by the inverted atoms into all spatial directions from its zero-signal value of $\gamma_\parallel D_p$.

The energy conservation condition (2.14) can be written in the form

$$G_T(\omega)|\beta_S|^2+G_R(\omega)|\beta_S|^2+\gamma_\parallel(D-D_p)=|\beta_S|^2 \quad (3.9)$$

for the below-threshold amplifier, where the gains are defined in (3.3) and (3.4). The reduction in spontaneous emission is thus exactly balanced by the energy needed to provide amplification of the input signal. Figure 6 shows the variations of the output signal fluxes and the change $\gamma_\parallel(D-D_p)$ in the spontaneous emission rate with signal detuning for $C=\frac{1}{2}$, where the laser cavity is assumed to be symmetrical with $\gamma_1=\gamma_2=\gamma_c$ and the input flux is given the value $|\beta_{\text{in}}|^2=|\beta_S|^2=\gamma_c n_s$. Note that the sum of the three contributions, corresponding to the left-hand side of (3.9), has the detuning-independent value of the right-hand side of (3.9).

The stability of the below-threshold state in the presence of an input signal is determined by the conditions given in

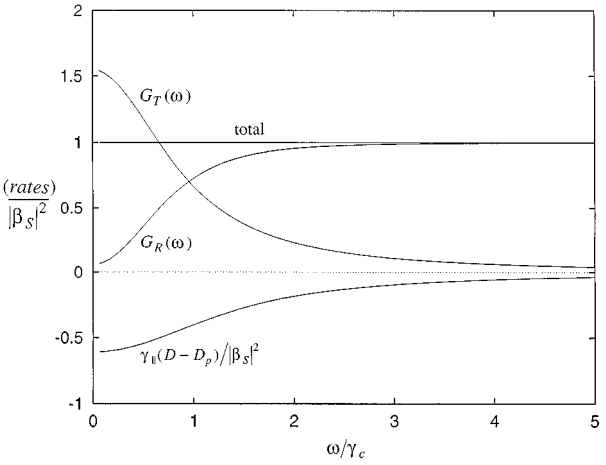

FIG. 6. Energy conservation in a below-threshold laser amplifier ($C=\frac{1}{2}$) with a symmetrical cavity, showing the variations of output fluxes and the change in spontaneous emission rate with signal detuning. The rates are normalized by the value of the input signal flux, chosen to be $|\beta_S|^2=\gamma_c n_s$, so that the output fluxes are expressed as gains. The sum of the three rates, shown by the horizontal line at ordinate 1, verifies the conservation of energy.

(2.39). It is evident from (2.32) that $D<D_0$ for the laser below threshold with $C<1$, and it is seen by inspection of (2.36) and (2.37) that the first two stability conditions are satisfied. A simple calculation with the forms of all three coefficients given in (2.36) to (2.38) shows that the third condition in (2.39) is also satisfied, and the state considered in this subsection is indeed stable.

IV. ABOVE-THRESHOLD LASER AMPLIFIER (SECOND-ORDER THEORY)

A. Equations of motion

In the normal state of the laser amplifier above threshold, where the strength of the input signal is insufficient to cause injection locking, the cavity field α and the population inversion D contain all of the terms given in (2.43) and (2.44) correct to second order in the input signal amplitude β_S. The equations of motion (2.9) and (2.10) can be separated into sets of equations in the zeroth, first, and second orders in β_S after substitution of the forms of solution (2.42)–(2.44). The components of the equations of motion that oscillate at different frequencies can also be separated out. The zeroth-order equations reproduce the results for the free-running laser given in Sec. II C.

Solution of the first-order equations produces the results

$$\alpha_S=i\{\omega^2+i\omega\gamma_\parallel C-\gamma_\parallel\gamma_c(C-1)\}\gamma_2^{1/2}\beta_S/\omega\mathscr{A}(\omega), \tag{4.1}$$

$$\alpha_I=-i\,\frac{2g^2\gamma_c\gamma_2^{1/2}\alpha_L^2\beta_S^*}{\omega\gamma_\perp\mathscr{A}^*(\omega)} =-i\,\frac{\gamma_\parallel\gamma_c(C-1)\gamma_2^{1/2}\beta_S^*\exp(2i\phi_L)}{\omega\mathscr{A}^*(\omega)}, \tag{4.2}$$

and

$$D_1=2\gamma_c\gamma_2^{1/2}\alpha_L^*\beta_S/\mathscr{A}(\omega), \tag{4.3}$$

where the denominator is

$$\mathscr{A}(\omega)=\omega^2+i\omega\gamma_\parallel C-2\gamma_\parallel\gamma_c(C-1) \tag{4.4}$$

and ϕ_L is the unknown phase of the field at the laser frequency

$$\alpha_L=|\alpha_L|\exp(i\phi_L). \tag{4.5}$$

The frequency ω in these expressions is the signal detuning from the unshifted laser frequency defined in (1.1), as the shift ω_L'' affects the satellite amplitudes and population inversion only in higher orders of the signal strength. The first form of α_I in (4.2) reflects the four-wave-mixing origin of this excitation at frequency $2\omega_L-\omega_S$ in the combination of two photons at the laser frequency and one at the signal frequency. The above first-order results have been derived previously [1].

The second-order part of the equation of motion (2.9) separates into three different frequency components

$$-i\omega_L''\alpha_L=(g^2/\gamma_\perp)(\alpha_L D_0''+\alpha_S D_1^*+\alpha_I D_1), \tag{4.6}$$

$$(\gamma_c-2i\omega)\alpha_{2S}=(g^2/\gamma_\perp)(\alpha_L D_2+\alpha_S D_1+\alpha_{2S}D_0), \tag{4.7}$$

and

$$(\gamma_c+2i\omega)\alpha_{2I}=(g^2/\gamma_\perp)(\alpha_L D_2^*+\alpha_I D_1^*+\alpha_{2I}D_0), \tag{4.8}$$

while the equation of motion (2.10) separates into two components

$$\gamma_\parallel C D_0''=-(2g^2/\gamma_\perp)\{(\alpha_L\alpha_L''^*+\alpha_L^*\alpha_L''+|\alpha_S|^2+|\alpha_I|^2)D_0 +\alpha_L(\alpha_S^*D_1+\alpha_I^*D_1^*)+\alpha_L^*(\alpha_S D_1^*+\alpha_I D_1)\} \tag{4.9}$$

and

$$(\gamma_\parallel-2i\omega)D_2=-(2g^2/\gamma_\perp)\{(\alpha_L\alpha_{2I}^*+\alpha_L^*\alpha_{2S}+\alpha_S\alpha_I^*)D_0 +(\alpha_L\alpha_I^*+\alpha_L^*\alpha_S)D_1+|\alpha_L|^2D_2\}. \tag{4.10}$$

These five complex equations provide solutions for the two real quantities ω_L'' and D_0'' and the four complex quantities α_L'', α_{2S}, α_{2I}, and D_2, and they can be obtained by straightforward but somewhat tedious algebra.

B. Injection locking

Consider first the second-order corrections to the parameters of the emission into the basic laser line. The solution for the shift in the frequency of this line can be written in the form

$$\frac{\omega_L''}{\gamma_c}=\frac{\gamma_\parallel\gamma_2^2[-\omega^2+2\gamma_\parallel\gamma_c(C-1)](C-1)}{\omega\mathcal{D}(\omega)}\,\frac{|\beta_S|^2}{\gamma_2|\alpha_L|^2}, \tag{4.11}$$

where

$$\mathcal{D}(\omega)=|\mathscr{A}(\omega)|^2=\omega^2\gamma_{\parallel}^2C^2+[\omega^2-2\gamma_{\parallel}\gamma_c(C-1)]^2. \tag{4.12}$$

It is seen that the frequency shift is negative, that is, away from the input signal frequency, for detunings greater than the frequency $[2\gamma_{\parallel}\gamma_c(C-1)]^{1/2}$ associated with relaxation oscillations [4]. However, the shift is otherwise positive, and this is the case for the parameter values assumed in the remainder of the paper. The positive shift obtained from (4.11) for detunings very much smaller than the relaxation oscillation frequency agrees with previous work [4].

The mean number of photons excited in the cavity at the shifted laser frequency is given by

$$|\alpha_L+\alpha_L''|^2\approx|\alpha_L|^2+\alpha_L\alpha_L''^*+\alpha_L^*\alpha_L'', \tag{4.13}$$

correct to second order in the input signal amplitude, where the solution for the second-order change in the laser field gives

$$\alpha_L\alpha_L''^*+\alpha_L^*\alpha_L''=-\{\omega^4+2\omega^2\gamma_{\parallel}[\gamma_{\parallel}C-\gamma_c(C-1)] +2[\gamma_{\parallel}\gamma_c(C-1)]^2\}\gamma_2|\beta_S|^2/\omega^2\mathcal{D}(\omega). \tag{4.14}$$

It is easily shown by rearrangement of terms that the expression in the curly brackets is positive for all values of the parameters. The mean photon number in the shifted laser line determined by (4.13) and (4.14) is thus reduced and the laser line is extinguished for a sufficiently large input signal flux $|\beta_S|^2$ or a sufficiently small detuning ω. The extinction of the laser line corresponds to the onset of the injection-locked state of the laser amplifier, and for a given input signal flux, the detuning at which the transition occurs according to the second-order theory is denoted ω_{IL}''.

These expressions for the second-order frequency shift and change in laser intensity simplify considerably for a class-A laser, where $\gamma_{\parallel}\gg\gamma_c$ and ω, and the approximate results in this case are

$$\frac{\omega_L''}{\gamma_c}=\frac{2\gamma_2^2\gamma_c(C-1)^2/\omega C^2}{\omega^2+[2\gamma_c(C-1)/C]^2}\frac{|\beta_S|^2}{\gamma_2|\alpha_L|^2}, \tag{4.15}$$

which is always positive, and

$$\alpha_L\alpha_L''^*+\alpha_L^*\alpha_L''=-\frac{2[\omega^2C+\gamma_c^2(C-1)^2]\gamma_2|\beta_S|^2/\omega^2C^2}{\omega^2+[2\gamma_c(C-1)/C]^2}. \tag{4.16}$$

The variation of the mean output photon flux at the shifted laser frequency with the input signal detuning, given by (4.13) and (4.16), is illustrated by the curves labeled L in Fig. 7 for two values of the input flux. As the flux is normalized by the output flux $2\gamma_c|\alpha_L|^2$ of the free-running laser, these curves all tend to the value unity for input detunings so large that the laser emission is unaffected by the input signal.

The detuning ω_{IL}'', for which injection locking occurs, determined by the condition for extinction of the laser line, is obtained from (4.13) and (4.16) in the form of a quadratic equation for $\omega_{IL}''^2$. Figure 8 shows the variation of this second-order injection-locking detuning with input flux, together with the laser frequency shift ω_L'' at the injection-locking point, obtained from (4.15). These figures again assume a symmetrical cavity and a normalized pumping rate $C=2$. It is seen that the injection-locking detuning frequency ω_{IL}'' and the laser frequency shift ω_L'' tend to the same value when the input signal flux is much smaller than the output flux of the free-running laser and the detunings are much smaller than the cavity decay rate γ_c. Approximate expressions in this case are

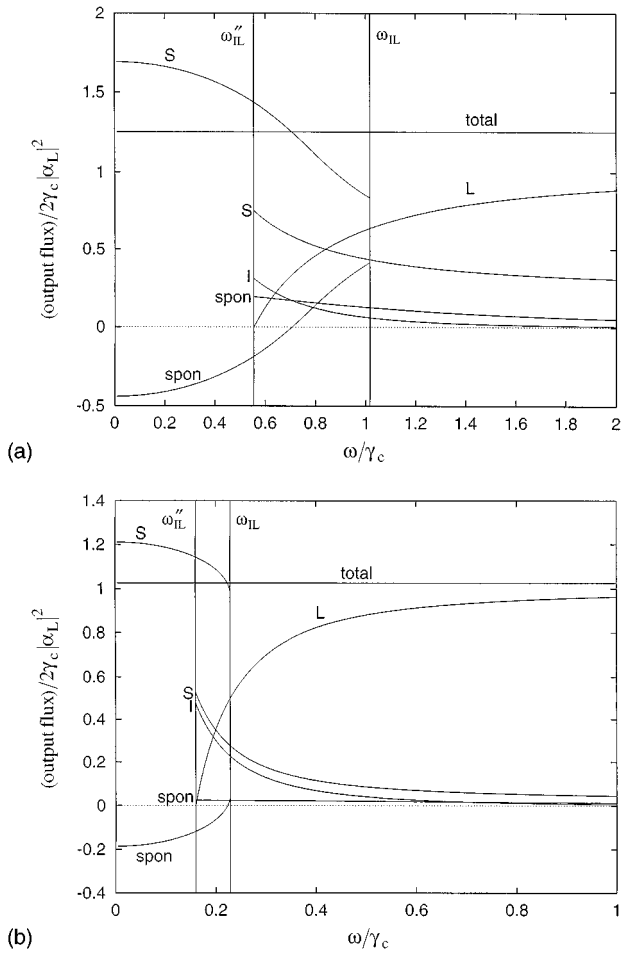

FIG. 7. Energy conservation in an above-threshold class-A laser amplifier ($C=2$) with a symmetrical cavity correct to second order in β_S, showing the variations with signal detuning of total output fluxes at the laser (L), signal (S), and image (I) frequencies and the change in spontaneous emission rate (spon), normalized by the output flux $2\gamma_c|\alpha_L|^2$ of the free-running laser. Results are shown for input signal strengths $|\beta_S|^2/\gamma_c|\alpha_L|^2$ equal to (a) 0.5 and (b) 0.05. The right-hand side of each part refers to the normal state of the laser amplifier and the left-hand side to the injection-locked state. The sums of the rates, shown by the lines (total) at ordinates $1+(|\beta_S|^2/2\gamma_c|\alpha_L|^2)$, verify the conservation of energy.

$$\frac{\omega_L''}{\gamma_c}=\frac{\gamma_2^2}{2\gamma_c\omega}\frac{|\beta_S|^2}{\gamma_2|\alpha_L|^2} \tag{4.17}$$

from (4.15) and

$$\frac{\omega_{IL}''}{\gamma_c}=\frac{\gamma_2}{\sqrt{2}\gamma_c}\left(\frac{|\beta_S|^2}{\gamma_2|\alpha_L|^2}\right)^{1/2} \tag{4.18}$$

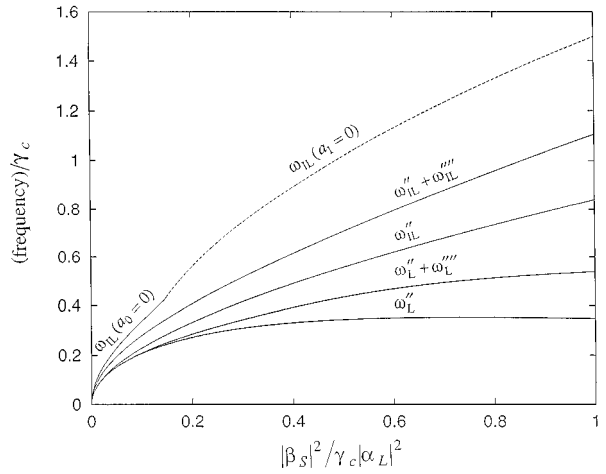

FIG. 8. Variations with input signal flux of the detuning for which injection locking occurs (upper three curves) and the laser frequency shift at injection locking (lower two curves), for a class-*A* laser with $C=2$ and a symmetrical cavity. The detunings ω''_{IL} and ω''''_{IL} are obtained from the second- and fourth-order theories of the normal state of the laser amplifier, respectively, while ω_{IL} is obtained from the theory of the injection-locked state. The laser frequency shifts ω''_L and ω''''_L are the contributions of second and fourth order in the input signal amplitude.

from (4.13) and (4.16). Substitution of ω''_{IL} for ω in (4.17) then produces the result $\omega''_L=\omega''_{IL}$.

A theory of injection locking similar to that outlined above was presented by Pantell [5] many years ago. As has been previously discussed [1], his neglect of the excitation of the cavity at the image frequency leads to results that are qualitatively valid, but they differ in detail from the above expressions. Thus, for example, his result for the output signal strength in the linear regime differs from that obtained from (4.1) by the absence of the factor of 2 in the denominator defined in (4.4) or (4.12) and his expression for the laser frequency shift is always negative. Similarly, his result for the detuning and input signal flux needed to produce injection locking differs from (4.18) by removal of the factor of $\sqrt{2}$. However, it should be emphasized that these second-order theories for the extinction of the laser line are in any case very approximate. As the injection-locking point is approached, satellite lines of progressively higher and higher order acquire significant strength from the laser line and the second-order theory tends to underestimate the detuning and overestimate the input signal flux needed to cause injection locking. A better account of the conditions at the injection-locking point is provided by a theory for the injection-locked state itself, and this forms the topic of Sec. VI.

C. Gain

The expressions (4.1) and (4.2) for the field amplitudes at the signal and image frequencies are unchanged when the theory is extended to second order in the input signal amplitude; the first modification of these linear forms occurs in the third-order theory presented in Sec. V. The linear gain of the above-threshold laser amplifier has been considered in detail in Ref. [1], and we summarize here the results for the transmission gain, so that they can be compared with the corresponding expressions in the injection-locked state. Thus, with the same definition as in (3.3), the transmission gains at the signal and image frequencies obtained from (4.1) and (4.2) are

$$G_{TS}(\omega)=\frac{\gamma_1\gamma_2}{\omega^2}\,\frac{\omega^2\gamma_\parallel^2C^2+[\omega^2-\gamma_\parallel\gamma_c(C-1)]^2}{\omega^2\gamma_\parallel^2C^2+[\omega^2-2\gamma_\parallel\gamma_c(C-1)]^2} \tag{4.19}$$

and

$$G_{TI}(\omega)=\frac{\gamma_1\gamma_2}{\omega^2}\,\frac{\gamma_\parallel^2\gamma_c^2(C-1)^2}{\omega^2\gamma_\parallel^2C^2+[\omega^2-2\gamma_\parallel\gamma_c(C-1)]^2}, \tag{4.20}$$

where the form of the denominator is taken from (4.12). These are the gains that would be measured by direct detection of the laser output spectrum, and they should be distinguished from the self-heterodyne gain derived and measured in [1], where the detected intensity is determined by the square of a linear superposition of the signal and image amplitudes.

The linear gains for a class-*A* laser simplify to

$$G_{TS}(\omega)=\frac{\gamma_1\gamma_2}{\omega^2}\,\frac{\omega^2+[\gamma_c(C-1)/C]^2}{\omega^2+[2\gamma_c(C-1)/C]^2} \tag{4.21}$$

and

$$G_{TI}(\omega)=\frac{\gamma_1\gamma_2}{\omega^2}\,\frac{[\gamma_c(C-1)/C]^2}{\omega^2+[2\gamma_c(C-1)/C]^2}. \tag{4.22}$$

The horizontal lines on the left-hand sides in Fig. 9 show some examples of the signal gain in transmission for two values of the input signal detuning.

D. Energy conservation

The solution of (4.6)–(4.10) for the second-order correction to the static population inversion is

$$D''_0=2\gamma_\parallel\gamma_2\gamma_cC|\beta_S|^2/\mathcal{D}(\omega). \tag{4.23}$$

The presence of the input signal thus produces an increase in the population inversion, in contrast to the reduction that occurs below threshold. Of course the conditions below threshold ensure that the energy needed for any amplification of the input signal must be found at the expense of the spontaneous emission, there being no other source of energy. For the laser above threshold, the laser photons provide the main source of energy, and a reduction in the part D_p-D_0 of the population inversion associated with the laser emission corresponds to an increase in the part D_0 associated with the spontaneous emission in all directions. For the class-*A* laser, the change in spontaneous emission rate obtained from (4.23) can be written

$$\gamma_\parallel D''_0=\frac{2\gamma_2\gamma_c|\beta_S|^2/C}{\omega^2+[2\gamma_c(C-1)/C]^2}, \tag{4.24}$$

and the variation of this quantity with detuning is shown by the curves labeled ''spon'' on the right-hand sides of Fig. 7.

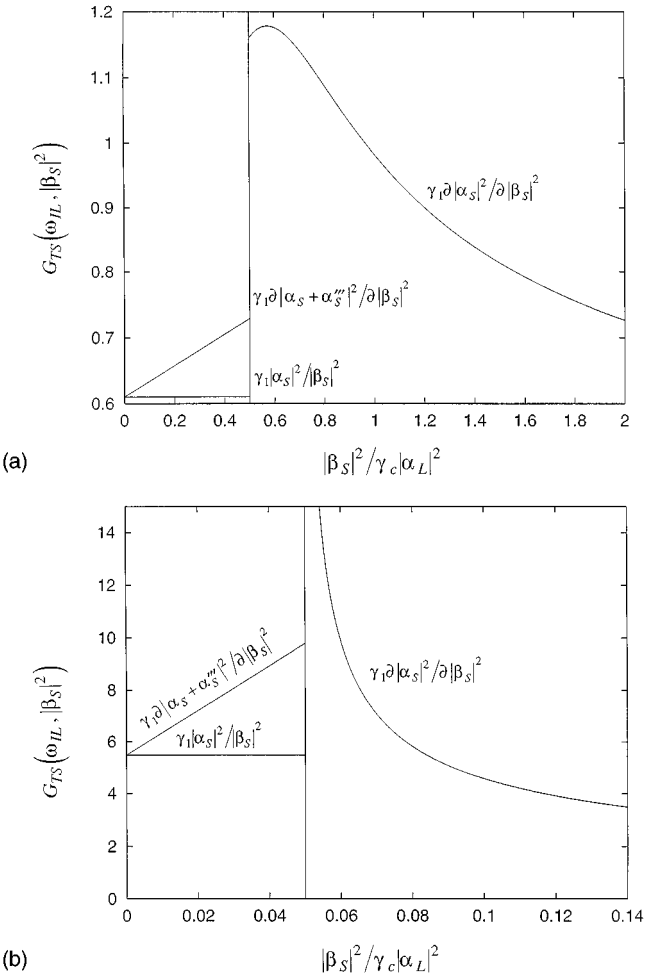

FIG. 9. Variation of differential transmission gain at the signal frequency with input signal flux for a class-*A* laser amplifier at detunings ω/γ_c equal to (a) 1.02 and (b) 0.23, the injection-locking frequencies ω_{IL}/γ_c for values of the normalized input flux $|\beta_S|^2/\gamma_c|\alpha_L|^2$ equal to 0.5 and 0.05, respectively. The lines to the left of the injection-locking points show the gains in the normal state, correct to zeroth and second orders in $|\beta_S|$, while the curves to the right show the gains in the injection-locked state.

The second-order quantities derived above are consistent with the energy conservation conditions expressed by (2.13) and (2.14). With an excitation of the laser cavity that now contains several frequency components, the cycle-averaged output fluxes are given by

$$\overline{|\alpha_{\text{out}}|^2}=\gamma_1\{|\alpha_L|^2+\alpha_L\alpha_L''^*+\alpha_L^*\alpha_L''+|\alpha_S|^2+|\alpha_I|^2\} \tag{4.25}$$

and

$$\overline{|\beta_{\text{out}}|^2}=\gamma_2\{|\alpha_L|^2+\alpha_L\alpha_L''^*+\alpha_L^*\alpha_L''+|\alpha_S|^2+|\alpha_I|^2\} -\gamma_2^{1/2}(\alpha_S\beta_S^*+\alpha_S^*\beta_S)+|\beta_S|^2, \tag{4.26}$$

correct to second order in β_S. It is straightforward to show with the use of (2.2), (4.1), (4.2), (4.14), and (4.23) that

$$\overline{|\alpha_{\text{out}}|^2}+\overline{|\beta_{\text{out}}|^2}+\gamma_\parallel D_0''=2\gamma_c|\alpha_L|^2+|\beta_S|^2, \tag{4.27}$$

and this is seen to agree with the energy conservation requirement (2.14) when the expression (2.23) with $D=D_0$ for the free-running laser output flux is used. The right-hand sides of Fig. 7 show the variations with detuning of the change in the spontaneous emission rate and the output fluxes in the laser, signal, and image lines, for the normal state of a class-*A* laser. It is seen that the sum of these quantities is always equal to the right-hand side of (4.27), independent of ω.

The remaining second-order quantities obtained by solution of (4.6)–(4.10) are the satellite amplitudes

$$\alpha_{2S}=g^2\gamma_2\gamma_c\{-4\omega^3-2i\omega^2\gamma_\parallel(2C+1) +\omega\gamma_\parallel[2\gamma_\parallel C+3\gamma_c(C-1)]+i\gamma_\parallel^2\gamma_c C(C-1)\} \times\alpha_L^*\beta_S^2/2\omega\gamma_\perp\mathscr{A}'(\omega)\mathscr{A}(\omega)^2, \tag{4.28}$$

$$\alpha_{2I}=-ig^4\gamma_2\gamma_c\{2\omega^3-i\omega^2(2\gamma_\parallel C+7\gamma_c)-5\omega\gamma_\parallel\gamma_c C +4i\gamma_\parallel\gamma_c^2(C-1)\}\alpha_L^3\beta_S^{*2}/\omega^2\gamma_\perp^2\mathscr{A}'^*(\omega)\mathscr{A}^*(\omega)^2 \tag{4.29}$$

and the amplitude of the population pulsation of frequency $2\overline{\omega}$

$$D_2=2g^2\gamma_2\gamma_c\{2\omega^3+i\omega^2(2\gamma_\parallel C+3\gamma_c)-3\omega\gamma_\parallel\gamma_c C -2i\gamma_\parallel\gamma_c^2(C-1)\}\alpha_L^{*2}\beta_S^2/\omega\gamma_\perp\mathscr{A}'(\omega)\mathscr{A}(\omega)^2, \tag{4.30}$$

where

$$\mathscr{A}'(\omega)=2\omega^2+i\omega\gamma_\parallel C-\gamma_\parallel\gamma_c(C-1). \tag{4.31}$$

The structure of the expression (4.28) for α_{2S} is similar to that of (4.2) for α_I and it reflects the origin of the satellite at frequency $2\omega_S-\omega_L$ in a four-wave-mixing process that involves two signal photons and one laser photon. By contrast, the expression (4.29) for α_{2I} has a different structure that reflects the origin of the satellite at frequency $3\omega_L-2\omega_S$ in a six-wave-mixing process that involves two signal photons and three laser photons. The square moduli of the amplitudes given by (4.28) and (4.29) determine the intensities of the second signal and image satellite lines, but these are of fourth order in β_S and they do not contribute to the second-order output flux expressions (4.25) and (4.26).

V. THIRD- AND FOURTH-ORDER THEORY

The second-order theory of the above-threshold laser amplifier outlined in Sec. IV is readily extended to higher orders in the input signal amplitude. We give here some results for the third- and fourth-order terms in the characteristics of the laser line and its satellites. These indicate how the description of the laser amplifier develops as progressively higher-order terms are included in the theory. Although yet higher-order terms could be evaluated, at least in principle, the calculations become very complicated, and they are not justified by the additional benefits to physical understanding.

Consider first the extension to third order, where the mean internal field in the laser cavity, given in second order by (2.43), expands to

$$\alpha=(\alpha_L+\alpha_L'')\exp[-i\omega_L t]+(\alpha_S+\alpha_S''')\exp[-i(\omega_L+\overline{\omega})t]$$
$$+(\alpha_I+\alpha_1''')\exp[-i(\omega_L-\overline{\omega})t]$$
$$+\alpha_{2S}\exp[-i(\omega_L+2\overline{\omega})t]$$
$$+\alpha_{2I}\exp[-i(\omega_L-2\overline{\omega})t]+\alpha_{3S}\exp[-i(\omega_L+3\overline{\omega})t]$$
$$+\alpha_{3I}\exp[-i(\omega_L-3\overline{\omega})t] \tag{5.1}$$

and the mean population inversion, given in second order by (2.44), expands to

$$D=D_0+D_0''+(D_1+D_1''')\exp(-i\overline{\omega t})$$
$$+(D_1^*+D_1'''^*)\exp(i\overline{\omega t})$$
$$+D_2\exp(-2i\overline{\omega t})+D_2^*\exp(2i\overline{\omega t})$$
$$+D_3\exp(-3i\overline{\omega t})+D_3^*\exp(3i\overline{\omega t}), \tag{5.2}$$

where the new terms are those with 3 subscripts or three primes. It is seen that the terms of first order in the input signal amplitude acquire additional third-order corrections and that new terms associated with the satellites at detunings $\pm 3\overline{\omega}$ from the shifted laser frequency ω_L appear.

The procedure is now the same as in Sec. IV, in that the above expressions for the cavity field and the population inversion are substituted into the equations of motion (2.9) and (2.10), which can then be separated into sets of equations corresponding to the different orders in β_S. The equations of the zeroth, first, and second orders in β_S are the same as before, but there are new third-order equations in sufficient quantity to determine all of the third-order amplitudes that occur in (5.1) and (5.2). The solutions are quite complicated in general, and we give here partial results only for class-A lasers, where $\gamma_\parallel \gg \gamma_c$ and ω, the signal detuning.

The third-order correction to the amplitude of the first signal satellite line is

$$\alpha_S'''=-g^2\gamma_2^{3/2}\gamma_c\{2\omega^4C^2(2C+1)+2i\omega^3\gamma_c C(C-1)$$
$$\times(C^2+2C+3)-5\omega^2\gamma_c^2C^2(C-1)^2$$
$$+2i\omega\gamma_c^3C(C-1)^3$$
$$-4\gamma_c^4(C-1)^4\}\beta_S|\beta_S|^2/\omega^3\gamma_\perp\gamma_\parallel C^5\not{\Lambda}(\omega) \tag{5.3}$$

and the change in the amplitude of the first image line is

$$\alpha_I'''=\frac{4g^2\gamma_c\gamma_2^{1/2}\alpha_L\beta_S^*\{\gamma_\perp\gamma_\parallel[\omega C-i\gamma_c(C-1)]\alpha_L''+2ig^2\gamma_c\alpha_L^2\alpha_L''^*\}}{\omega\gamma_\perp^2\gamma_\parallel^2[\omega C-i2\gamma_c(C-1)]^2}$$
$$+\frac{4g^4\gamma_c\gamma_2^{3/2}\{\omega^3C-3i\omega^2\gamma_c(C^2-1)-\omega\gamma_c^2(C-1)(5C-4)+i\gamma_c^3(C-1)^2\}\alpha_L^2\beta_S^*|\beta_S|^2}{\omega^2\gamma_\perp^2\gamma_\parallel^2C^4\not{\Lambda}^*(\omega)}, \tag{5.4}$$

where

$$\not{\Lambda}(\omega)=\{\omega^2+[2\gamma_c(C-1)/C]^2\}\{\omega+i[2\gamma_c(C-1)/C]\}^2$$
$$\times\{\omega+i[\gamma_c(C-1)/C]\} \tag{5.5}$$

and α_L'' is determined by (4.14). The change D_1''' in the first-order population pulsation, the amplitudes α_{3S} and α_{3I} of the two new satellites that occur in the third order of the injected signal amplitude, and the amplitude D_3 of the third-order modulation of the population pulsation have all been determined [21], but their detailed forms are not needed for the present discussions.

The change (5.3) in the signal amplitude modifies the linear transmission gain (4.21) by the addition of a nonlinear contribution. The nonlinear gain is best expressed in differential form as

$$G_{TS}(\omega,|\beta_S|^2)=\frac{\partial|\alpha_{\text{out}}|^2}{\partial|\beta_{\text{in}}|^2}$$
$$=\gamma_1\frac{\partial}{\partial|\beta_S|^2}\{|\alpha_S|^2+\alpha_S\alpha_S'''^*+\alpha_S^*\alpha_S'''\}, \tag{5.6}$$

correct to order $|\beta_S|^2$, and this reduces to the definition of the linear gain in (3.3) if the fourth-order terms on the right-hand side of (5.6) are neglected. The inclined lines on the left-hand sides in Fig. 9 show the differential gains obtained from (5.6) with the use of (4.1) and (5.3).

The extension to fourth order in the amplitude of the input signal is performed in a similar fashion. Thus the mean internal field α of the laser acquires terms additional to those in (5.1) that oscillate at frequencies $\omega_L\pm 4\overline{\omega}$ and there are fourth-order corrections to the laser field (denoted α_L'''') and to the satellite fields α_{2S} and α_{2I}. The population inversion D acquires terms additional to those in (5.2) that pulsate at frequencies $\pm 4\overline{\omega}$ and there are fourth-order corrections to the static term and to the terms that pulsate at frequencies $\pm 2\overline{\omega}$. The laser frequency itself acquires a fourth-order correction, so that (2.40) is replaced by

$$\omega_L=\omega_{L0}+\omega_L''+\omega_L'''' \tag{5.7}$$

and the definition (2.41) of the signal detuning from the shifted laser line is replaced by

$$\overline{\omega}=\omega-\omega_L''-\omega_L''''=\omega_S-\omega_L=\omega_L-\omega_I. \tag{5.8}$$

The detuning for which injection looking occurs also acquires a fourth-order correction, denoted ω_{IL}'''', and this is

determined by the condition for extinction of the laser line, obtained by generalization of the expression (4.13) for the mean number of photons in the cavity at the shifted laser frequency

$$|\alpha_L+\alpha_L''+\alpha_L''''|^2\approx|\alpha_L|^2+\alpha_L\alpha_L''^*+\alpha_L^*\alpha_L''+\alpha_L\alpha_L''''^*+\alpha_L^*\alpha_L''''+|\alpha_L''|^2=0. \tag{5.9}$$

The detailed expressions for the various fourth-order quantities have been calculated [21], but they are quite complicated and instead of giving their explicit forms, we show their effects by means of some numerical examples. Thus Fig. 8 shows the effects of addition of the fourth-order corrections to both the laser frequency shift and the injection-locking frequency. It is seen that the correction to the laser frequency shift is small for the signal input fluxes towards the left-hand end of the axis, but that the correction is relatively large for the larger input fluxes and truncation of the theory at the fourth-order terms does not provide reliable values for the shift in this region. The fourth-order correction to the injection-locking frequency is seen to lie between about one-fifth and one-third of its second-order value over most of the illustrated range of input signal fluxes, again indicating that the expansion of the laser equations of motion in power series of the input flux requires additional terms in order to obtain accurate results close to the injection-locking point.

The effects of the third- and fourth-order terms in the laser and satellite amplitudes and in the population pulsation are illustrated by Fig. 10, which shows the variations with signal detuning of the contributions to the total output flux from the laser amplifier, again for $C=2$ and for a symmetrical cavity. The curves can be compared with the second-order results shown on the right-hand sides of Fig. 7. The total emitted fluxes are unchanged, in conformity with the requirements of energy conservation, but they are redistributed between the different components. For a given value of ω/γ_c, the output flux at the laser frequency is always reduced, in accordance with the larger values of the detuning for which the transition to the injection-locked state occurs in the fourth-order theory. The outputs at the second image, and particularly the second signal, frequencies are small in fourth order.

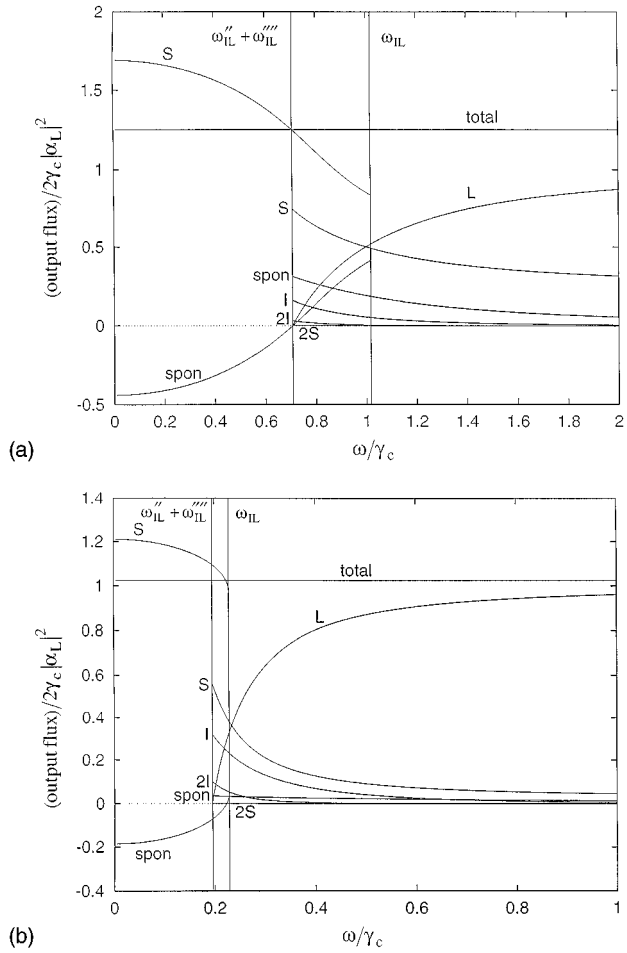

FIG. 10. Energy conservation in an above-threshold class-A laser amplifier with $C=2$ and a symmetrical cavity, showing the variations with signal detuning of the output fluxes at the laser (L), signal (S), and image (I) frequencies and the change in spontaneous emission rate (spon), correct to fourth order in β_S. The rates are normalized by the output flux $2\gamma_c|\alpha_L|^2$ of the free-running laser and results are shown for input signal strengths $|\beta_S|^2/\gamma_c|\alpha_L|^2$ equal to (a) 0.5 and (b) 0.05. The sums of the rates, shown by the lines at ordinates $1+(|\beta_S|^2/2\gamma_c|\alpha_L|^2)$, verify the conservation of energy.

VI. INJECTION-LOCKED LASER AMPLIFIER

The injection-locked state of the laser amplifier is simpler than its normal, or unlocked, state because the extinction of the laser line removes the multiple satellite spectrum. The field in the laser cavity thus has only the single component of frequency ω_S, illustrated in the final part of Fig. 3, and the population inversion D loses its pulsating components. The theory outlined in Sec. II D therefore applies, with C now taken to be larger than unity. The injection-locked state thus resembles the laser amplifier below threshold, treated in Sec. III, but important differences occur on account of the high level of excitation of the signal mode in the laser cavity. The theory of injection-locking in the limit of small input signals is described by Siegman [4], and Tredicce *et al.* [14] have considered some aspects of the stability of the state. Here we determine the main features of the injection-locked state in greater detail, including its stability, for comparison with the other regimes of operation of the laser amplifier.

The single-component cavity field, whose form is given by (2.26), has an amplitude $|\alpha_S|$ determined by solution of (2.33); the same cubic equation also occurs in the theory of Pantell [5], which is valid in the injection-locked state since there is no excitation at the image frequency. The static population inversion is given by (2.32). The continuous curves in Figs. 11 and 12 show the results of some numerical calculations of the mean-square intracavity field and the population inversion as functions of the input signal flux, for several values of detuning from the unshifted laser frequency. It is seen that both of these quantities have three different solutions for the smaller values of signal detuning [6], but only single solutions occur for the larger detunings. The solutions for $\omega=0$ and their stability have been considered previously [7]. All of the solutions satisfy the inequality

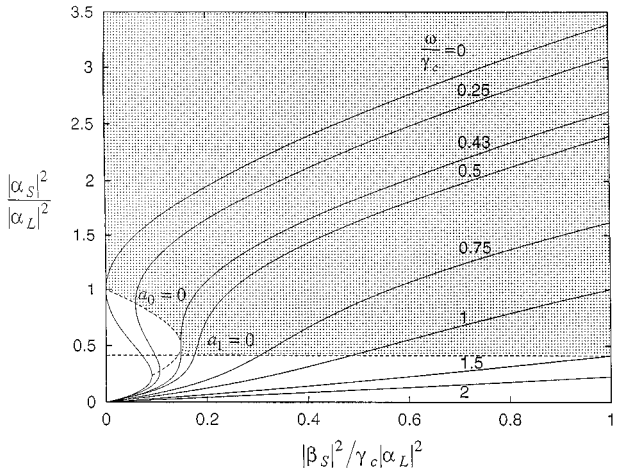

FIG. 11. Variation of the normalized intracavity mean photon number with normalized input signal flux in the injection-locked state of a class-*A* laser amplifier with $C=2$ for the values of detuning ω/γ_c indicated. The broken curves are the boundaries of the stability region shown by the shaded area.

(2.31) and the mean-square cavity field and population inversion take the simple values given in (2.34) when this is satisfied as an equality. The continuous curves in Figs. 11 and 12 are valid for both class-*A* and class-*B* lasers, irrespective of the value of $\gamma_\parallel/\gamma_c$.

The shaded regions in Figs. 11 and 12, bounded by the broken curves, indicate the parameter ranges for which the injection-locked state is stable. These stability regions are determined by Hurwitz's theorem and their boundaries are determined by the conditions (2.39) expressed as equalities. Consider first the boundary determined by the condition $a_0=0$, which is represented by the broken curves on the left of the figures. It is apparent from (2.36) that this condition is also independent of the ratio $\gamma_\parallel/\gamma_c$, and the same boundary applies for all class-*A* and class-*B* lasers. The condition $a_0=0$ has no simple analytic form in general (although an

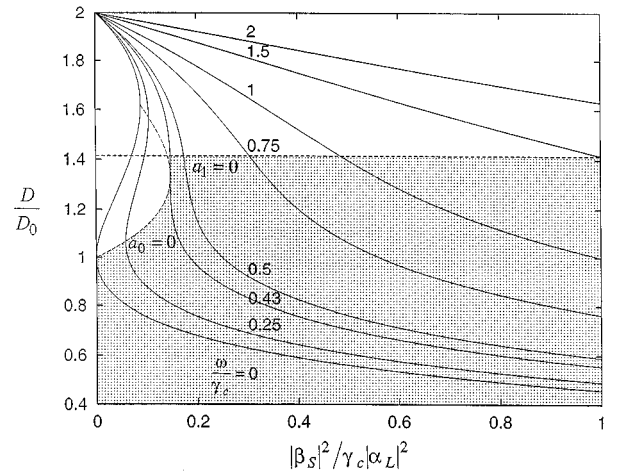

FIG. 12. Variation of the normalized population inversion with normalized input signal flux in the injection-locked state of a class-*A* laser amplifier with $C=2$ for the values of detuning ω/γ_c indicated. The broken curves are the boundaries of the stability region shown by the shaded area.

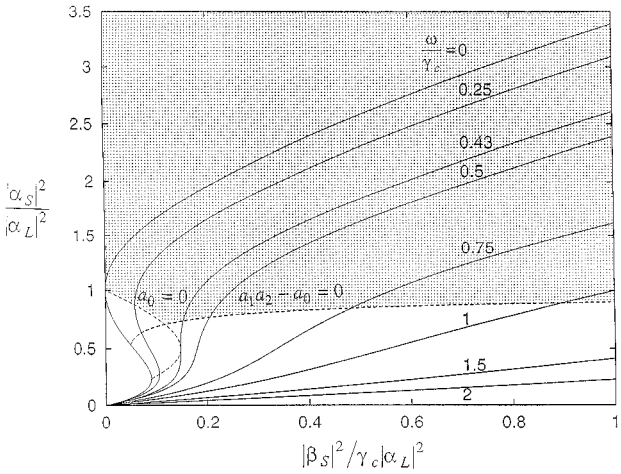

FIG. 13. Same as Fig. 11, but for a class-*B* laser amplifier with $\gamma_\parallel/\gamma_c=0.2$, as appropriate for CO_2.

approximation for small input signal fluxes is discussed later in the section) and the corresponding broken curves in Figs. 11 and 12 are obtained numerically. They are seen to intersect the continuous curves at points where these have vertical tangents, and indeed the condition $a_0=0$ can be rederived by differentiation of (2.33) or, symbolically,

$$a_0=0\Leftrightarrow\frac{\partial|\alpha_S|^2}{\partial|\beta_S|^2}=\infty. \tag{6.1}$$

By contrast, the boundaries determined by the conditions $a_1=0$ and $a_2a_1=a_0$ obtained from (2.39) do depend on the ratio $\gamma_\parallel/\gamma_c$ and they are different for the different classes of laser.

Consider first the class-*A* laser, where $\gamma_\parallel\gg\gamma_c$, and the condition $a_1=0$ from (2.37) takes the limiting form

$$1-\frac{D}{D_0}+\frac{|\alpha_S|^2}{n_s}=0. \tag{6.2}$$

The $a_1=0$ stability boundaries obtained with the use of (2.32) are thus

$$\frac{|\alpha_S|^2}{n_s}=\sqrt{C}-1,\quad \frac{D}{D_0}=\sqrt{C}. \tag{6.3}$$

These straight-line boundaries are shown in Figs. 11 and 12. The remaining stability boundary condition $a_2a_1=a_0$ is seen from (2.36)–(2.38) to be identical to $a_1=0$ to leading order in $\gamma_\parallel/\gamma_c$ and the second and third conditions in (2.39) are degenerate for the class-*A* laser.

The straight-line boundaries do not occur for the class-*B* laser, where all of the bounding curves of the stability regions must be obtained numerically. The continuous curves in Figs. 13 and 14 show the same variations of mean-square intracavity field and population inversion with input signal flux as Figs. 11 and 12, but with shaded stability regions and their broken boundary curves drawn for a ratio $\gamma_\parallel/\gamma_c$ appropriate to a CO_2 laser. It is seen that the stability conditions (2.39) now give rise to three different boundary curves in principle, although the condition $a_1=0$ has no real solutions

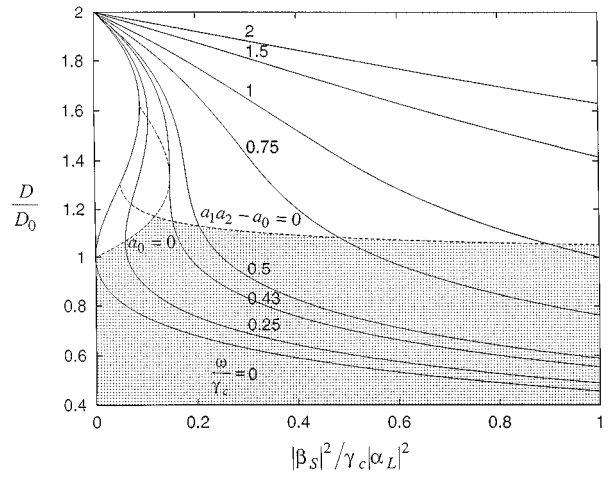

FIG. 14. Same as Fig. 12, but for a class-*B* laser amplifier with $\gamma_\parallel/\gamma_c = 0.2$, as appropriate for CO_2.

for the chosen parameter values. The broken curves for $a_0 = 0$ are unchanged from those in Figs. 11 and 12.

The maximum detuning frequency for which the injection-locked state persists, denoted ω_{IL}, is a function of the input signal flux that can be obtained from the equations for the boundaries of the stability region, with the mean-square intracavity field and population inversion eliminated by the use of (2.32) and (2.33). The calculation must be performed numerically for the curve $a_0 = 0$, but for a class-*A* laser the limiting forms in (6.3) can be used for the curve $a_1 = 0$ and the resulting relation obtained from (2.33) is

$$\frac{\omega_{IL}^2}{\gamma_c^2} = \frac{|\beta_S|^2}{\gamma_c n_s}\frac{1}{\sqrt{C}-1} - (\sqrt{C}-1)^2, \tag{6.4}$$

where the laser cavity is assumed symmetrical ($\gamma_1 = \gamma_2 = \gamma_c$). The right-hand side of (6.4) becomes negative for a sufficiently small input signal, and it appears that an imaginary injection-locking frequency could be obtained. However, it is straightforwardly shown from (2.36) and (6.3) that the stability boundaries $a_0 = 0$ and $a_1 = 0$ intersect at the input signal strength and frequency given by

$$\frac{|\beta_S|^2}{\gamma_c n_s} = 2(\sqrt{C}-1)^3, \quad \frac{\omega_{IL}}{\gamma_c} = \sqrt{C}-1, \tag{6.5}$$

and the $a_1 = 0$ boundary becomes redundant before the right-hand side of (6.4) becomes negative. The frequency ω_{IL} puts limits on the maximum value of detuning and minimum value of input signal field for which the injection-locked state is stable. It thus provides a value of the detuning for injection locking that can be compared with the values obtained from the theory of the normal state.

The results for a class-*A* laser are shown in Fig. 8, where the composite curve labeled ω_{IL} is constructed numerically from the boundary condition $a_0 = 0$ for smaller values of the input signal flux and analytically from the boundary condition $a_1 = 0$ given by (6.4) for the larger values of input signal flux. It is seen that the injection-locking frequency ω_{IL} obtained from the condition for the existence of a stable injection-locked state is larger than the value $\omega_{IL}'' + \omega_{IL}''''$ obtained in the fourth-order theory from the condition (5.9) for the vanishing of the field excitation at the laser frequency in the normal state of the laser amplifier. However, it is clear from Fig. 8 that the fourth-order terms in the theory of the normal state make significant corrections to the second-order frequencies, and it is expected that the sixth- and higher-order terms will produce further increases in the injection-locking frequency as the emission at the laser frequency suffers further reductions by transfer into the growing number of satellite lines. More accurate treatments of the normal state should thus bring the two curves of injection-locking frequency closer together.

The identical left-hand sides of Figs. 7 and 10 show some typical results for the variations with signal detuning of the output flux at the signal frequency and the change $\gamma_\parallel(D - D_0)$ in the spontaneous emission rate from the free-running laser value, obtained by numerical solution of the cubic equation (2.33) for $|\alpha_S|^2$. A comparison of the different right-hand sides of these figures shows how the apparent regions of coexistence of the injection-locked and normal states of the laser amplifier shrink as higher-order terms are included in the theory of the normal state. The change in spontaneous emission rate in the injection-locked state from the free-running laser value can be either positive or negative in accordance with the solutions of (2.30) for $D - D_0$, and the occurrence of positive values at the larger detunings accords with the increase in spontaneous emission predicted by the theory for the normal state.

The signal gain in transmission is nonlinear in the injection-locked state, and it is again appropriate to work with the differential gain defined in (5.6), where the output flux $\gamma_1|\alpha_S|^2$ is now obtained by solution of the cubic equation (2.33). Some typical numerical results are shown in the sections of the curves of Fig. 9 for input signal fluxes greater than the value for which injection locking occurs. It is seen by comparison with Fig. 11 that the gain remains finite at the $a_1 = 0$ injection-locking boundary, as in Fig. 9(a), but that infinite differential gain occurs on the $a_0 = 0$ boundary, as in Fig. 9(b), in accordance with the infinite slope condition (6.1) on this boundary. The onset of injection locking generally leads initially to an increase in the gain, compared to the gain in the normal state shown on the left-hand sides in Fig. 9, but higher-order terms in the normal-state theory could again lead to closer agreement between the values on either side of the injection-locking transition. For the injection-locked state with very high input fluxes, where $|\beta_S|^2 \gg \gamma_c n_s$, the approximate solution of (2.33) given in (3.2) remains valid and the gain approaches the limiting value given by (3.6).

The condition for energy conservation in the injection-locked state resembles that in the below-threshold laser amplifier, given by (3.9), as signal amplification or attenuation can only be compensated by reduction or increase in the spontaneous emission. The condition can be written in the form

$$|\alpha_{\text{out}}|^2 + |\beta_{\text{out}}|^2 + \gamma_\parallel(D - D_0) = 2\gamma_c|\alpha_L|^2 + |\beta_{\text{in}}|^2, \tag{6.6}$$

where the first two terms on the left-hand side represent the total output flux at the signal frequency. The energy conservation is illustrated by the numerical results in Figs. 7 or 10,

where each frame shows a sum total of the contributions to the rate of emission of energy that remains equal to the same constant value throughout the normal and injection-locked states of the laser amplifier, in accordance with (4.27) and (6.6).

The properties of the injection-locked state derived here can be compared with those found in the limit of a weak input signal [4], where $\gamma_2|\beta_S|^2 \ll |\alpha_L|^2$. The injection locking in this case occurs at small signal detunings with $\omega \ll \gamma_c$, and it is seen from Figs. 11–14 that only the stability boundary condition $a_0 = 0$ need be considered. With the use of (2.32) and (2.36), this condition can be approximated to obtain

$$\frac{|\alpha_S|^2}{|\alpha_L|^2} \approx 1 - \frac{C^2}{2(C-1)^2} \frac{\omega^2}{\gamma_c^2} \tag{6.7}$$

and

$$\frac{D}{D_0} \approx 1 + \frac{C}{2(C-1)} \frac{\omega^2}{\gamma_c^2}, \tag{6.8}$$

correct to second order in ω/γ_c. These forms can now be substituted into (2.30) to obtain an approximation to the injection-locking frequency

$$\frac{\omega_{IL}^2}{\gamma_c^2} \approx \frac{|\beta_S|^2}{\gamma_c|\alpha_L|^2} + \frac{C^2}{4(C-1)^2} \left(\frac{|\beta_S|^2}{\gamma_c|\alpha_L|^2} \right)^2, \tag{6.9}$$

with the cavity again assumed symmetrical. This expression provides a good approximation to the curve for ω_{IL} in Fig. 8 for small input signals, and in combination with (6.7) and (6.8) it reproduces the $a_0 = 0$ boundaries in Figs. 11–14 in the same regime. Previous derivations for small input signal fluxes have included only the first terms on the right-hand sides of the above three results [4,14]. Figures 7(b) and 10(b) correspond to small input signals and provide a more detailed description, compared to Fig. 29.4 of Ref. [4], of the behavior close to the injection-locking point.

VII. CONCLUSIONS

The calculations reported in this paper have two main aims in the development of the understanding of the properties of a class-*A* or class-*B* laser with an injected signal. The first aim is the extension of previous calculations of the effects of the input signal on the output fields of the laser beyond the regime of linear amplification. In the normal, or unlocked, state of the laser amplifier this is accomplished by the expansion of the dynamical variables of the laser in power series in the amplitude of the input signal. The laser equations of motion can then be solved progressively to increasing orders in the signal amplitude, and we have given results up to fourth order. It has been shown that increasing orders correspond to the excitation of an output spectrum that contains increasing numbers of pairs of signal-image satellites centered symmetrically on the laser line and separated by integer multiples of the detuning of the input signal from the laser frequency. The pulsations in the population inversion likewise acquire higher harmonics of the frequency detuning. These contributions are produced by higher-order nonlinearities in the coupling of the optical waves and the population pulsations in the laser cavity, and the nth image satellite and the $(n+1)$th signal satellite are generated by $2(n+1)$-wave-mixing processes. The emission of output flux in the satellite lines occurs at the expense of the output flux in the laser line, which is reduced from its free-running value. The satellites grow in intensity and the laser line weakens as the input signal flux is increased and as the signal detuning from the laser line is reduced. We have also evaluated the shifts in the frequency of the laser line that occur when terms of the second and fourth orders in the amplitude of the input signal are included.

The second aim is the comparison of the conditions for injection locking obtained by an increase in input signal strength, or a reduction in the signal detuning, in the normal state of the laser amplifier and from the stability of the injection-locked state itself. The former approach was developed by Pantell [5], who identifies the injection-locking point from the condition that the emission at the laser frequency is extinguished. We have improved on this earlier work by inclusion of the first image satellite in the linear theory and by inclusion of the second signal and image satellites in the nonlinear theory. The inclusion in the theory of more satellites produces enhanced transfer of energy away from the laser line and thus causes the transition to the injection-locked state to occur for smaller input signal strength and larger detuning. This approach to the theory of injection locking can only be approximate, as it becomes algebraically impractical to include all of the significant satellites in the immediate vicinity of the injection-locking point.

The injection-locked state itself is amenable to a more exact treatment, as the cavity field is excited at the single frequency of the input signal and its mean-square amplitude satisfies a cubic equation. We have determined the ranges of signal strength and detuning for which the state is stable by solutions of the cubic equation and evaluation of the Hurwitz conditions for the stability of its roots. These calculations are mainly numerical, given the basic cubic form of the amplitude equation, but some of the stability boundary conditions can be written as analytic expressions, particularly for the class-*A* laser or for small input signal fluxes. Thus the relation between the input signal detuning and strength at the injection-locking point of a class-*A* laser is largely expressible in analytic form. The detuning for a given signal strength obtained from this latter theory is consistently larger than that obtained from the former approach, which is to be expected, given the approximations inherent in the power-series expansion, but we have shown that the two results for the detuning become closer as higher-order terms are included in this expansion. The properties of the injection-locked state and its transition to or from the normal state derived here agree with previous work in the limit of small input signal strength [4].

We have evaluated the transmission gains, or losses, at the frequency of the input signal that are achieved in the various states of the laser amplifier, namely, below threshold, the normal state above threshold, and the injection-locked state, and for each state we have determined the natures of the energy redistributions that are needed to source the amplification or attenuation. For the below-threshold and injection-locked states, the energy balance for amplification

or attenuation is taken from or given to the spontaneous emission in all directions and indeed there is no other source or sink of energy for these states. The situation is more complex for the normal state of the laser amplifier, where the presence of an amplified input signal produces an increase in the spontaneous emission in all directions, together with axial emission into other satellites of the laser line, all of which are sourced by reductions in the emission at the shifted laser frequency.

It has not been possible to compare the detailed predictions of the injection-locking theory presented here with experimental results, as the measurements currently available do not provide sufficient numerical data for evaluation of the various expressions. However, the general scheme shown in Fig. 3 for the development of the laser spectrum with reduction in the detuning of the input signal is in good agreement with measurements on the CO_2 laser [3]. Thus the growth of the satellite spectrum and falloff in laser intensity were observed as the detuning was reduced, leading to the extinction of all except the signal contribution at the injection-locking point. Such measurements, made, for example, with a signal of fixed intensity, can tune the signal through the frequency ω_{L0} of the free-running laser, from positive to negative detunings, so that the states of the system pass from normal to injection locked and back to normal. The natures of the transitions between states, as the equilibrium of the initial state becomes unstable, could thus be observed and compared with the predictions of theory for such quantities as the satellite intensities, transition signal strengths and detunings, and laser frequency shifts. It would also be interesting to observe the predicted change in the sign of this frequency shift as the detuning of the injected signal passes through the relaxation oscillation frequency of a class-*B* laser. It is hoped that the calculations reported here will stimulate more detailed experimental work, leading to a better understanding of the injection-locked state and the transitions between it and the normal state of the laser amplifier.

ACKNOWLEDGMENTS

We are indebted to Dr. Mike Harris of the Defense Research Agency for helpful discussions. J.J. thanks the Iranian Ministry of Culture and Higher Education for financial support.

[1] R. Loudon, M. Harris, T. J. Shepherd, and J. M. Vaughan, Phys. Rev. A **48**, 681 (1993).
[2] J.-M. Liu and T. B. Simpson, IEEE J. Quantum Electron. **30**, 957 (1994).
[3] G. N. Pearson, M. Harris, C. A. Hill, J. M. Vaughan, and A. M. Hornby, IEEE J. Quantum Electron. **31**, 1064 (1995).
[4] A. E. Siegman, *Lasers* (University Science Books, Mill Valley, CA, 1986).
[5] R. H. Pantell, Proc. IEEE **53**, 474 (1965).
[6] M. B. Spencer and W. E. Lamb, Phys. Rev. A **5**, 884 (1972).
[7] L. A. Lugiato, Lett. Nuovo Cimento **23**, 609 (1978).
[8] D. K. Bandy, L. M. Narducci, and L. A. Lugiato, J. Opt. Soc. Am. B **2**, 148 (1985).
[9] D. K. Bandy, L. A. Lugiato, and L. M. Narducci, in *Instabilities and Chaos in Quantum Optics*, edited by F. T. Arecchi and R. G. Harrison (Springer, Berlin, 1987), p. 73.
[10] H. G. Solari and G.-L. Oppo, Opt. Commun. **111**, 173 (1994).
[11] H. Haken, *Light*, Vol. 2, *Laser Light Dynamics* (North-Holland, Amsterdam, 1985).
[12] N. B. Abraham, L. A. Lugiato, and L. M. Narducci, J. Opt. Soc. Am. B **2**, 7 (1985).
[13] F. T. Arecchi, in *Instabilities and Chaos in Quantum Optics* (Ref. [9]), p. 9.
[14] J. R. Tredicce, F. T. Arecchi, G. L. Lippi, and G. P. Puccioni, J. Opt. Soc. Am. B **2**, 173 (1985).
[15] M. J. Collett and C. W. Gardiner, Phys. Rev. A **30**, 1386 (1984).
[16] W. H. Louisell, *Quantum Statistical Properties of Radiation* (Wiley, New York, 1973).
[17] M. Sargent, M. O. Scully, and W. E. Lamb, *Laser Physics* (Addison-Wesley, Reading, MA, 1974).
[18] See, for example, R. Loudon, *The Quantum Theory of Light* (Clarendon, Oxford, 1983).
[19] See, for example, I. N. Bronshtein and K. A. Semendyayev, *A Guidebook of Mathematics* (Deutsch, Frankfurt, 1971).
[20] R. Adler, Proc. IRE **34**, 351 (1946).
[21] J. Jahanpanah, Ph.D. thesis, University of Essex (unpublished).